Published in final edited form as:
Biomaterials. 2012 February ; 33(5): 1323–1335. doi:10.1016/j.biomaterials.2011.10.034.

Inducing Alignment In Astrocyte Tissue Constructs By Surface Ligands Patterned On Biomaterials

Fanwei Meng[a], **Vladimir Hlady**[b], and **Patrick A. Tresco**[a]

[a]The Keck Center for Tissue Engineering, Department of Bioengineering, University of Utah, Salt Lake City, UT 84112, USA

[b]Department of Bioengineering, University of Utah, Salt Lake City, UT 84112, USA

Abstract

Planar substrates with patterned ligands were used to induce astrocyte alignment whereas substrates with uniform fields of ligand were used to produce random cell orientation. DRG neurons plated on top of oriented astrocyte monolayers exhibited directional outgrowth along aligned astrocytes, demonstrating that purely biological cues provided by the oriented astrocytes were sufficient to provide guidance cues. Antibody blocking studies demonstrated that astrocyte associated FN played a major mechanistic role in directing engineered neurite extension. Our results show that nanometer level surface cues are sufficient to direct nerve outgrowth through an intervening organized astrocyte cell layer. In other studies, we showed that patterned ligands were able to transmit organization cues through multiple cell layers to control the overall alignment of an astrocyte tissue construct, demonstrating how natural scar tissue may develop in situ into potent barriers. In such constructs the spatial organization of astrocyte derived FN maintained its organizational anisotropy throughout the thickness of multilayered astrocyte constructs. These in vitro studies suggest possible roles for such constructs as bridging substrates for neuroregenerative applications.

Keywords

astrocyte; extracellular matrix; axonal regeneration; anisotropy; 3-D culture; glial scar

1. Introduction

The ability of astroglia to guide neuronal pathfinding during development, *in vitro* and following injuries is well established. During development, astroglia provide directional information to pioneering axons by organizing into glial frameworks or boundaries at specific periods [1–6]. In addition, available evidence indicates that regenerating axons extend long distances following longitudinally aligned glial cells [7–11]. *In vitro*, various studies have shown that astrocytes and their secreted extracellular matrix (ECM) support neurite outgrowth of a variety of neuronal cell types [12–16]. In addition to acting as a permissive substrate, astrocytes also guide neurite extension through depositing inhibitory ECM [17–19].

Correspondence to: Patrick A. Tresco.

Given the knowledge that astroglia serve as guidepost cells during development, as well as, following injuries and support neurite outgrowth *in vitro*, understanding how regenerating axons interact with astroglia may shed light on developing new therapeutic approaches to reconstruct parts of the damaged nervous system or to bypass the disorganized astroglial scar [20–22]. To facilitate functional recovery, severed and/or spared sprouting axons must reinnervate specific and not random targets so methods that allow control over the trajectory of regenerating axons may provide technology to enhance functional recovery [23].

Several groups are studying how to engineer oriented glial substrates to study the underlying cellular and molecular mechanisms by which glial cells guide neuronal pathfinding [24–27]. It was previously demonstrated that oriented, engineered astrocyte substrates are useful for enhancing directed neurite outgrowth [25,26,28]. In one approach, topographical grooves and indentations in growth culture substrates have been used to orient astrocyte morphology [25,26,29]. Nerve cells plated on top of the directionally oriented astrocytes extend neurites in the same direction as the underlying oriented astrocyte monolayers [25,26]. However, using such an approach, it is not clear whether the architectural features themselves are responsible for the directional orientation of the overlying neurons as grooved substrates alone are effective in directing neurite elongation [30,31].

To better elucidate the mechanisms involved in astrocyte mediated neuronal outgrowth, planar substrates with patterned nanometer-level anisotropic guidance cues were produced with soft lithographic methods in which continuous lanes of laminin (15μm wide) were interspersed by continuous lanes of untreated glass (15μm wide). We used this approach to exclude the influence of physical undulations on directing neurite trajectories, and examined how engineered astrocyte constructs affect the directional outgrowth of adjacent regenerating neurites, as well as, how they affected the orientation of adjacent astrocytes in thick tissue engineered constructs.

2. Materials and Methods

2.1 Micropatterning device fabrication

Polydimethylsiloxane (PDMS, R-2615, Nusil) contact printing stamps were designed using software L-edit and fabricated in the University of Utah Microfabrication laboratory. Stamps were designed to have anisotropic continuous lanes (15 μm wide) interspersed with continuous bare coverslip surfaces (15 μm wide) in order to provide directional information to align astrocytes.

Photolithographic masks of the designed pattern were fabricated using a micropattern generator (Electromask). Resulting masks were used directly as molds to produce PDMS stamps. PDMS two component kit was mixed in a 1:10 ratio, vacuumed treated to remove bubbles till no bubbles were observed, poured into a mold and then cured at 100°C for 30 mins. The cured PDMS stamps were peeled off against the mold and cut into approximately 1×1.5 cm^2 blocks. PDMS stamps were immersed in hexane overnight to remove residual uncured PDMS prior used for protein pattern transferring.

2.2 Microcontact printing

Glass coverslips were cleaned by rinsing with acetone, isopropanol followed by double distilled deionized (DD) water, then sonicated for 15 mins and autoclaved. 10 μl laminin solution (LN, 400 μg/ml in sterile PBS; Sigma) was applied to each PDMS stamp and covered by a coverslip to help the solution spread the entire stamp surface for 25 mins. After adsorption, stamps were rinsed with sterile DD water and briefly dried under a nitrogen stream. LN adsorbed stamps with and without a lane pattern were brought into contact with clean coverslips and then removed to generate both isotropic and anisotropic protein pattern.

2.3 Astrocyte and DRG isolation and preparation

Purified primary rat postnatal astrocytes were isolated as previously described [32]. Cerebral cortices from postnatal Day 1 (P1) Sprague-Dawley rats were dissected out with meninges removed, then minced and digested (1.33% collagenase, 30 mins, Worthington Biochemical) followed by 0.25% trypsin treatment (30 mins, Worthington Biochemical). The cells were triturated and suspended in DMEM/F12 medium (Invitrogen) with 10% fetal bovine serum (FBS, Atlantic Biological). The dissociated cells were plated in 75 cm^2 flasks. After one week, purified astrocytes were obtained by overnight shake-off at 175 rpm. Dorsal root ganglion neurons (DRG) were isolated from P1 rats as previously described [23]. Individual neurons were removed from their location near the spinal column. Then the attached nerve roots were removed and the ganglia neurons were suspended in a trypsin/collagenase (0.25%/0.33%) mixture for 30 mins. The tissue was then triturated. The resulting cell suspension was centrifuged, suspended in 1 ml DMEM/F12 plus 50 μl of DNase. Then dissociated DRG neurons were plated on astrocytes monolayers on various patterns in DMEM/F12 with 10% FBS.

2.4 Astrocyte and DRG culture

Purified astrocytes were seeded on LN lanes patterned or onto homogeneous fields of LN surfaces at a density of 17,300 cells/cm^2 in serum free medium (SATO−) over the first 4–6 hrs and then switched to 10% FBS for the remainder of the 4 day period to create confluent oriented and randomly, organized astrocytes monolayers, respectively. Medium was changed every other day. To produce fixed oriented and randomly, organized astrocytes monolayers, astrocytes were cultured as described above and fixed by immersion in 4% paraformaldehyde for 15 mins after 4 days in culture. After fixation, cell layers were rinsed with sterile PBS once and then immersed in DMEM/F12 medium at 37°C for 2 days to remove and deactivate residual aldehyde groups generated during the fixation process. Fresh medium was changed everyday.

DRG neurons were seeded on both live and fixed astrocytes monolayer cultures (both oriented and randomly, organized) at a density of 580 DRG neurons/cm^2 in 10% FBS supplemented with 10 ng/ml 2.5S nerve growth factor (NGF; Invitrogen). The co-cultures were cultured for an additional 48 hrs and then treated with 4% paraformaldehyde for 15 mins and then stored in PBS with azide.

Purified astrocytes were seeded on patterned (anisotropic) and unpatterned (isotropic) surfaces at a density of 52,000 cells/cm^2 with serum free medium (SATO-) over the first 4–6 hrs and switched to 10% FBS for 2 days to create the first confluent, oriented and random astrocyte monolayers, respectively. Then, the seeding process was repeated every other day with 52,000 cells/cm^2 in 1.5 ml 10% FBS. Half of the culture medium in each well was replaced with fresh medium the next day following cell seeding. The seeding process was repeated for 3–4 times to create multilayered astrocyte cultures, which were then fixed using 4% paraformaldehyde.

2.5 Anti-FN antisera blocking experiment

Fixed oriented astrocyte monolayers were treated with mouse anti-FN antisera (45 μg/ml, Sigma) for 3 hrs then rinsed with sterile PBS prior to adding dissociated DRG neurons. DRG neurons were seeded at a density of 580 DRG neurons/cm^2 in 10% FBS, supplemented with 10 ng/ml 2.5S NGF. DRGs were cultured for an additional 48 hrs and treated with 4% paraformaldehyde for 15 mins and then stored in PBS with azide. Untreated, fixed oriented astrocyte monolayers served as controls. There were four repeat experiments for each group.

2.6 Immunohistochemistry and image acquisition

For intracellular antigens, fixed cultures were treated with 0.05% triton X-100 in PBS for 5 mins and rinsed with PBS three times. No triton was applied for the extracellular matrix molecular immunohistochemical detection. Fixed cell layers were blocked with 4% goat serum and 0.1% sodium azide in PBS for 1 hr and incubated with primary antisera against glial fibrillary acidic protein (GFAP, DAKO, 1:1000), neurofilament (NF160, Sigma, 1:500), laminin (LN, Sigma, 1:500), cellular fibronectin (FN, Sigma, 1:500), chondroitin sulfate proteoglycan (CS-56, Sigma, 1:500) and neural cell adhesion molecule (NCAM, Sigma, 1:500). Appropriate conjugated secondary antibodies (Molecular Probes) were applied at dilution of 1:500 except for GFAP (1:1000). All antibodies were diluted in 4% goat serum with 0.1% azide and applied for 24 hrs at room temperature. Fixed cell layers were rinsed with PBS three times both after primary and secondary antibody application. DAPI (10 μM; Molecular Probes) was used for all cell nuclei visualization. Coverslips were mounted with Fluoromount–G (Southern Biotechnology). Images were acquired using a Nikon epifluorescence microscope equipped with a CCD camera or using an Olympus FVX laser scanning confocal microscope.

2.7 Astrocyte orientation analysis

The orientation of elliptical DAPI+ astrocytes cell nuclei was used to determine astrocyte orientation as well as their overall appearance. For astrocytes cultured on unpatterned LN surface, the vertical axis of each image was chosen as the reference axis. For astrocytes cultured on the patterned LN substrate, the long axis of the printed LN lane pattern was used as the reference axis for calculating cell orientation. A built-in function of ImagePro (Media Cybernetics) was used to generate elliptical outlines for all cell nuclei and the angle made between the long axis of each elliptical mask and the designated axis of the image was calculated. Nuclei that were cut off by the edge of images and clusters of nuclei that overlapped, which the program could not distinguish and recognize were manually removed from the data set. Each measurement was placed into a data bin of plus or minus 10° off the designated axis of each image. Angle bins ranged from −90° to 90° with 0° being parallel to the designated vertical axis of each image. Four random images were taken from each coverslip and there were four repeats for each condition (oriented and random).

2.8 Neurite length and alignment quantification

NF-160 antibody was used to visualize neuronal cell bodies and their processes. Neurite angle and length measurement were conducted using NIH Image J software. Directed length was measured and defined as the vector length of each neurite growing in the direction of interest. To calculate the directed length, a straight line was first drawn from the tip of the neurite to the cell soma. Then the directed length of each neurite was calculated by multiplying the length of the straight line by the cosine of the angle made between the straight line and the direction of interest. A designated axis of each image was chosen as the direction of interest for DRGs grown on astrocytes monolayers cultured on unpatterned substrates (both live and fixed) whereas the long axis of the LN lane pattern was used for DRGs grown on oriented astrocyte layers (both live and fixed).

Orientation of neurite outgrowth was quantified by measuring the angle between the straight line drawn from the tip of the neurite to the cell soma and the reference axis. Each measurement was placed into a data bin of 10° ranging from −90° to 90° with 0° being parallel to the reference axis. There were three repeats for each condition (live random, fixed random, fixed oriented and live oriented).

2.9 Multilayered astrocyte analysis

2D fast fourier transform (FFT) has been used to analyze anisotropy in cells [24,62]. Multilayered astrocyte cultures (random and aligned) were stained for FN and the spatial distribution of astrocyte derived FN was used as an indicator for cellular orientation. Confocal microscopy was used to image through the thickness of the multilayered astrocyte cultures. 2D FFT was applied on the z-stack images of both random and aligned multilayered cultures using NIH Image J software. The “Oval Profile” plug-in was used to determine radial sums over the 2D FFT image from 0° to 360° with discrete sampling of every 10°. These data were summarized so that the sum is unity. As the 2D FFT is symmetrical, only data points from 0° to 180° were used. It should be noted that the FFT image was first rotated 90° counterclockwise because the results of the FFT yield frequencies orthogonal to those in the original image. The anisotropy index was determined by the cell orientation distributions extracted from the 2D FFT [62]. The anisotropy index was determined by dividing the maximum value of the orientation distribution with the expected distribution value at that angle for a perfectly isotropic sample. Three random images were taken from each multilayered astrocyte cultures and there were three independent repeats.

2.10 AFM

The height in nanometers of stamped LN patterns was analyzed using a commercial AFM (Dimension 3000, Digital Instruments) in the University of Utah Microfibrication laboratory using the tapping mode.

2.11 Statistical analysis

All quantitative data were reported as the mean ± standard deviation or as a frequency distribution. One way ANOVA was used to compare the means. Astrocyte morphological orientation distributions and neurite angle distributions were analyzed for differences using a chi square test for independence. The relationship between astrocyte and DRG alignment was also assessed using a Pearson’s correlation coefficient. Two-tailed student t-test was used to pair-wise compare for anisotropy of multilayered astrocyte cultures. p-values < 0.05 were considered statistically significant.

3. Results

3.1 Astrocyte orientation on printed LN pattern

Microcontact printing (Fig. 1A) was used to generate continuous LN lanes of 15 μm width interspersed with continuous lanes of untreated glass strips of 15 μm width (Fig. 1C). Clean coverslips stamped with a homogenous LN field (Fig. 1B) were used to evaluate the ability of anisotropic LN lanes to direct astrocyte orientation. The height of the stamped LN lanes was approximately 5 nm as measured by AFM using tapping mode (Fig. 1D and E). Primary P1 astrocytes cultured on the printed LN pattern exhibited an elongated morphology that followed the underlying LN lanes 6 hrs after plating and the oriented morphology was maintained through out the whole culture period (Fig. 2G, H and I). Astrocytes cultured on the homogenous LN fields had no preferred directional orientation (Fig. 2A, B and C). A second cytoskeletal marker, actin, was used to confirm the orientation of astrocytes cultured on either isotropic LN fields or anisotropic LN lane pattern. When seeded on LN lanes, the orientation of actin microfilaments was closely associated with the observed morphological orientation of the cells (Fig. 2J, K and L). No preferred orientation of actin was observed on isotropic surfaces (Fig. 2D, E and F). These observations demonstrated a haptotactic influence of the anisotropic LN substrate distribution on the guidance behavior of astrocytes.

Confluent astrocytes (both aligned and random) were formed four days after initially seeding.

Astrocyte alignment on both patterned and homogeneous LN field (unpatterned) surfaces was quantified. The nuclei of oriented astrocytes exhibited elliptical morphology with their long axis oriented parallel to the underlying LN lane pattern, whereas equal proportions of astrocyte orientation on unpatterned surfaces fell within any particular angle bin, indicating random orientation on the homogenous LN field (Fig. 2M). Approximately 81% of the cells were aligned within 20 degrees of parallel to the long axis of underlying lane pattern (Fig. 2N). The difference between the two groups was significant (Chi Square Test for Independence, $p < 0.05$). The data demonstrated that nanometer level guidance cues can influence the morphology and directional bias of astrocytes on planar substrates.

3.2 Neurite outgrowth directionality

A close association was found between the orientation of overlying DRG neurite outgrowth trajectory and the morphological orientation of the underlying astrocytes. The direction of neurite outgrowth was generally in a direction parallel to the aligned astrocytes (Fig. 3C). In general, when DRGs were put on top of random astrocytes (cultured on LN field), no overall preferred orientation of neurite outgrowth was found (Fig. 3A). DRGs were also cultured on both fixed random and fixed oriented astrocytes cultures to assess whether simply the presence and the spatial distribution of non-diffusible factors (e.q. ECM proteins and cell surface bound ligands) derived from astrocytes were principally responsible for the guidance behavior. Similarly, neurite outgrowth exhibited strong alignment on the fixed, oriented astrocytes cultures (Fig. 3D). Again, no directional biased neurite outgrowth was found on fixed random astrocytes cultures (Fig. 3B). The 3D reconstructed confocal images (flipped around the Y-axis of a series z-stack images) demonstrated that although neurites penetrated into the astrocyte culture they rarely if ever reached the plane of the top of the coverslip, suggesting the observed guided neurite outgrowth was purely biological mechanism associated with the orientation of the astrocytes (Fig. 3E and F). Similar to the orientation distribution pattern of the random astrocytes cultures, neurite outgrowth angles were near uniformly distributed on both live and fixed random astrocytes cultures (Fig. 4A and B). By contrast, approximately 89% of neurite angles on both live and fixed oriented astrocytes were within 20 degrees of the long axis of LN lane pattern (Fig. 4C and D). The neurite angle distribution was significantly different between random and oriented astrocyte groups (Chi Square Test for Independence, $p < 0.05$). Overall, the relationship between the orientation of astrocytes and that of neurite outgrowth exhibited a strong correlation (Pearson's correlation coefficient > 0.87).

3.3 Oriented astrocytes direct outgrowth of neurites

In an attempt to determine the relationship between neurite trajectory and outgrowth length, the directed outgrowth of neurites parallel to the long axis of LN lanes (both live and fixed) and that of neurites parallel to a designated axis on random astrocytes (both live and fixed) was calculated. DRG outgrowth on oriented astrocytes resulted in greater directed outgrowth where 370% and 280% increase of directed length were seen on live and fixed oriented astrocytes, respectively than that on fixed random astrocytes, respectively. When compared to live random astrocytes, the increase of directed outgrowth dropped to 250% and 190% respectively (Fig. 5A). There was a significant difference in the directed length comparison between any two conditions (fixed random, live random, fixed oriented and live oriented, one-way ANOVA, $p < 0.05$). The distribution of directed neurite length on four conditions was evaluated and it was found the maximum value of directed neurite length increased gradually from fixed randomly organized, live randomly organized, fixed oriented to live

oriented astrocytes (Fig. 5B). These results indicated that the alignment as well as the viability of astrocytes affected directed length of neurite trajectories.

3.4 ECM expression of astrocytes and neurite outgrowth

Immunofluorescent staining with antisera against astrocyte associated FN, CSPG, LN and NCAM all revealed a spatial arrangement parallel to the long axis of LN lanes at a certain degree on the oriented astrocyte monolayers (Fig. 6B, D, F, and H). The parallel spatial distribution was the most evident with FN, which formed fibrillar bundles and was closely associated with the underlying stamped LN pattern (Fig. 6B, colocalization data of FN and LN lanes not shown). Similarly, the CSPG expression pattern also delineated the underlying printed LN lane pattern; however, it was not as distinct as FN and no fibrillar structure of CSPG was seen (Fig. 6D). NCAM is a cell membrane associated adhesion molecule expressed on astrocyte surface and its expression pattern seemed to outline the astrocytes cell membrane (Fig. 6F). Although the general pattern of NCAM on aligned astrocytes appeared to follow the long axis of printed LN lanes, we didn't see the similar fibrillar structure as we observed for FN. In order to investigate the distribution pattern of astrocytes derived LN, fibronectin lanes (400 μg/ml, Invitrogen) was patterned on the underlying substrate. The anisotropic nature of oriented astrocytes derived LN was the least obvious. (Fig. 6H). The spatial pattern of immunostaining of all four extracellular matrix molecules on random astrocytes revealed no preferred orientation (Fig. 6A, C, E and G). Although the overall pattern of FN on random astrocytes was not organized, small patches appeared organized where we observed that neurite outgrowth followed these oriented ligands (Fig. 6A arrow). Neurite outgrowth on oriented astrocytes didn't seem to be affected by the CSPG distribution and the neurites were found to extend through areas of both high and low level of CSPG expression (Fig. 6D). This phenomenon was also seen with neurites grown on random astrocytes cultures (Fig. 6C), suggesting CSPG derived from astrocytes in our culture conditions might have a weak inhibitory effect on neurite outgrowth that could be overwhelmed by other permissive guidance cues. The expression patterns of randomly organized astrocytes derived NCAM and LN showed no preferred directionality (Fig. 6E and G). The fact that neurites were found to be following with linear arrays of FN expressed on the oriented astrocytes as well as on the random astrocytes when these bundles oriented locally suggested a principle role of astrocytes derived FN in guiding neuronal pathfinding.

3.5 FN as a guiding ligand

Among all astrocyte derived insoluble ligands investigated, the anisotropic nature of FN suggests it might act as the most distinct path guiding ligand as revealed by indirect immunohistochemical reactions (Fig. 6B). Thus, we decided to examine what role that FN plays in interactions with DRG neurite outgrowth. DRG neurons were cultured on fixed oriented astrocyte cultures with or without anti-FN antisera treatment. There was more than 82% of neurites oriented within 20 degrees of the long axis of the underlying LN lanes on untreated fixed oriented astrocyte monolayers (Fig. 7A), whereas following anti-FN antisera treatment, the number of neurites oriented within 20 degrees dropped to 46% (Fig. 7B). There was a statistical difference between untreated and treated groups (Chi Square Test for Independence, $p<0.05$). This result suggested that astrocyte derived FN is a potent guiding ligand for DRG neuronal pathfinding.

3.6 Surface cues influence tissue organization

Following the first astrocyte layer reached confluence on either unpatterned (LN field) or patterned surface (LN lane pattern), additional astrocyte seedings were applied on top of the first layer and so on to investigate if the first aligned astrocyte monolayer was capable of transmitting the directional cues to subsequent cell layers and manipulate the organization of the overlying cell layer organization. Astrocyte derived FN was used as an indicator for

cellular orientation as it was shown that the anisotropy of FN on aligned astrocyte monolayers was most conspicuous parallel to astrocyte alignment (Fig. 6B). Both random and aligned, multilayered astrocyte cultures were mechanically separated from the coverslips using forceps. No preferred spatial organization of FN of randomly organized, multilayered astrocyte cultures was observed (Fig. 8A). On the contrary, the cellular alignment was preserved when astrocytes were repeatedly seeded on the aligned astrocyte monolayers (Fig. 8B). The orientation distribution of FN within the randomly organized, multilayered astrocytes maintained unbiased (Fig. 8C) whereas the FN distribution of aligned, multilayered astrocytes peaked around 90 degrees (Fig. 8D, parallel to the printed LN lanes). The anisotropy index further demonstrated that the preserved anisotropy of the aligned, multilayered astrocyte cultures (Fig. 8E). DAPI staining showed the multilayered structure of astrocyte cultures following multiple seedings (Fig. 8F). Reconstructed 3D confocal images also confirmed that the anisotropic organization of FN was distributed throughout the thick, multilayered astrocyte structure (Fig. 8G). This result demonstrated that surface guidance cues can be transmitted to overlying cell layers via the directional information carried by the spatial distribution of ligands present on an apical surface of the previous cell layer.

4. Discussion

Findings of this study demonstrated that the alignment of cultured astrocytes can be controlled by the anisotropic orientation of biomaterial surface ligands that are only a few nanometers in height. Further, spatially oriented astrocytes are capable of directing neuronal outgrowth from their apical surfaces, as well as, controlling the orientation of multiple astrocyte cell layers that are orders of magnitude larger than the initial templating ligands. This approach provides an opportunity to investigate the molecular mechanism by which astrocytes guide neuronal pathfinding in the absence of other interfering cues, such as topographical undulations as introduced by grooved guidance substrates [25,26,29].

We also demonstrated that the spatial organization of astrocyte derived insoluble factors is sufficient to direct neurite outgrowth grown on featureless surfaces showing that purely biological mechanisms are sufficient to guide tissue level organization. Our immunohistochemical analysis further suggested the involvement of linear arrays of astrocyte associated FN as a principle organizational mechanism. Together, these in vitro studies suggest an approach to create a multilayered-tissue construct with oriented morphology that could be useful in regenerative medicine.

Astrocytes, as a major glial cell type in the CNS, have been recognized as supportive substrates for neuronal growth through the secretion of diffusible neurotrophic factors and the expression of such insoluble permissive factors as ECM proteins, cell adhesion and cell surface ligands [11,12,14,33]. Studies have demonstrated that axons tend to follow the orientation of surrounding astroglial cells [7–11] and suggest that the formation of glial cell based tracts or boundaries precedes and guides neuronal pathfinding during CNS development [1–6,17–19].

However, following CNS injury, along with upregulation of a variety of inhibitory molecules [34–38,61], the disrupted extracellular milieu is accompanied by the formation of a disorganized glial scar that is also recognized as a major impediment to axonal regeneration [20–22]. Recently, the beneficial roles of reactive astrocytes after CNS injury have been revealed where they are involved in functional recovery and modulation of inflammatory cells [39]. Therefore strategies that maintain such positive contributions of reactive astrocytes while also providing directional information to constrain axonal regeneration trajectory may be useful clinically.

In our studies, the alignment of astrocytes was achieved by patterning nanometer level LN molecules as surface guidance cues on otherwise planar substrates. Patterned substrates have been shown to control cell orientation and function [40,41] and ECM proteins patterned in different shapes can affect the polarization of cell internal organization and future cell division axis [42,43]. The observed elongated morphology of astrocytes might be manifested through the interaction between the chemisorbed LN lanes and such ECM receptors as dystroglycan (DG) and integrin β1 that are found on astrocytes. Each of these receptors has been shown to regulate astrocyte attachment and actin organization in response to LN [44,45].

Previously several groups have shown that aligned astrocytes can direct neurite outgrowth. These approaches used grooved substrate topography on the order of hundreds of nanometers to hundreds of microns [25,26,29]. Thus, in these studies it is unclear whether neurite outgrowth was affected by the surface undulations of the grooved substrates [30]. Previously, we reported that when the R.M.S roughness of the substrate is below 45nm, grooved substrates failed to direct astrocyte orientation [25]. Therefore, the observed alignment of astrocytes on a planar surfaces printed with nanometer level surface cues (~5nm) indicates that the biological aspects of astrocyte orientation alone is sufficient to direct oriented neurite outgrowth in the absence of mechanical cues that could influence neurite trajectories via a different mechanism.

In this study, neurites were found to follow the alignment of underlying astrocytes (live and fixed), indicating that nanometer level surface cues on a planar bridging substrate are sufficient to affect the directional outgrowth of adjacent neural tissue through an intervening astrocyte layer. The astrocyte/meningeal cell interface is thought to be a barrier to axonal regeneration due to the fact that axons tend to stay on top of astrocytes and unwilling to across the boundary [46]. However, it has been shown that oriented meningeal cell layers support and enhance directed neurite outgrowth [47]. Therefore it would be interesting to see whether such a regeneration barrier could be overcome by inducing organization to these two major cellular components of the glial scar.

The length of directed neurite outgrowth was found to be a function of both the viability and orientation of underlying astrocytes since DRG neurites grown on fixed astrocyte monolayers lack of the neurotrophic factors released from astrocytes [33] and glial cell alignment has been shown to enhance directed neurite outgrowth [24,25,28]. This result suggests that a simple approach with organized, nanometer level surface cues on a CNS implanted bridging device may be used to organize the reactive astrocyte layer that encapsulates the implant,, and could be used to affect the trajectory of regenerating axons at the device surface.

The fact that neurites still grow parallel on fixed oriented astrocytes demonstrated that the spatial distribution of ECM proteins and/or cell surface bound ligands derived from astrocytes are sufficient to guide neurite extension. It was proposed by Tessier-Lavigne and colleagues that ECM proteins act as short range cues to guide growth cone extension [48] and a great number of ECM proteins and/or surface bound ligands have been demonstrated to affect neurite outgrowth trajectory [11,12,14,18,19,49–51].

Permissive and/or repulsive ligands immobilized on culture substrates in different geometries effectively guide outgrowth [50,52–54]. Therefore, one potential molecular mechanism by which oriented astrocytes govern the directionality of neuronal pathfinding is through the display of a network of ECM and/or surface bound ligands that mediate neuron-astrocyte interaction and provide directional information. DRG neurites grown on astrocytes aligned on a planar surface provides an opportunity to investigate the molecular mechanism

without the interference of other physical guidance mechanisms. Our results suggest that one could engineer artificial bridging devices through mimicking the spatial arrangement of these insoluble ligands displayed on oriented astrocytes.

DRG neurites were found making direct contact and closely associated with the continuous array of astrocyte derived FN, suggesting the potential role of FN in guiding neurite outgrowth. This close association between neurites and astrocyte associated FN was also observed previously where DRGs were grown on astrocytes aligned by grooved substrates [25]. In the present study, the direct role of astrocyte associated FN in guiding neurite outgrowth was strengthened due to the fact that no other mechanical guidance cues were contributing to the alignment of neurites.

Indeed, FN has been demonstrated to be critical for sensory axonal regeneration in adult rat corpus callosum [11] and to modulate neurite outgrowth [50]. However, DRG neurites were found not always making direct contact with astrocyte associated FN. We speculate that after receiving guidance information, neurites might be able to maintain outgrowth trajectory for a certain amount of time or distance traveled before they acquire new information due to the intrinsic stiffness of the trailing axon [31]. Therefore, while not always making direct contact with FN, neurites maintained parallel outgrowth. Still, this observation does not rule out the involvement of other ligands on the astrocyte surface in guiding neurite extension, such as NCAM [14]. However, the fact that the majority of neurites were not able to maintain directional outgrowth following anti-FN antisera treatment did demonstrate that astrocyte derived FN is a potent mechanism for guiding neurite outgrowth.

The observation that neurite growth was not affected by the level of CSPG expression can be explained in many ways. For example, the different sulfation pattern of glycosaminoglycans (GAG) chains has been shown to render CSPG distinct properties, either permissive or inhibitory [55,56]. The other possibility is that in our culture system the CSPG exerted inhibitory signals were overridden by other astrocyte derived permissive molecules [36]. The spatial distribution of astrocytes derived NCAM and LN did not appear to exhibit the same conspicuous anisotropic orientation as observed for FN. Their expression pattern suggested that they might be directing neurite outgrowth in a way different than FN by providing a permissive substrate that neurites prefer to extend on.

It has been suggested that cells lose alignment on patterned surfaces once the thickness of the cell/tissue layers goes beyond 20–40 μm [57]. However, in the current study, we demonstrated that the alignment of astrocytes within a multilayered structure can be maintained for at least 30 μm in thickness in a fixed specimen, which under hydrated conditions is likely much thicker. It will be interesting to see if this behavior is cell type specific. It also will be interesting to investigate how thick of the multilayered structure could become in which alignment is still preserved.

While many studies have demonstrated the repulsive nature of various scar-associated ligands in inhibiting axonal regeneration [58–60], very few studies have suggested how scar tissue may develop. In the current study, we demonstrate that astrocyte alignment can be transmitted through multiple cell layers to control the organization of a tissue construct, potentially via the directional cues carried by a network of spatially organized, astrocyte associated cell surface receptors and ECM ligands. Likewise our data suggests that disorganized astrocytes likely transmit their lack of organization, which likely contributes to the development of the dense inhibitory scar tissue that inhibits regeneration *in vivo* following injury.

5. Conclusion

Our studies performed totally in vitro show that the manner in which biomaterial bound surface ligands are presented affects the spatial organization of a population of cells at a biomaterial surface. Moreover, such organized patterns of surface ligands can strongly influence the directional outgrowth of neurons interacting with the surface of an organized astrocyte cell layer, as well as being transmitted through multiple cell layers to control the organization of a tissue construct. The results suggest that axonal regeneration can be facilitated following injuries if an organized glial framework is provided at a biomaterial surface. The results of our in vitro studies also suggest a biological mechanism by which a disorganized glial framework can develop into inhibitory scar tissue following injury, and conversely how an organized astrocyte framework could be engineered for use in spinal cord injury repair.

Acknowledgments

The authors thank Elena Budko, M.D., for assistance and thoughtful discussion. We also thank Brian Baker for his help for fabricating microprinting device. We acknowledge funding support from NIH 5R01NS57144.

References

1. Cummings DM, Malun D, Brunjes PC. Development of the anterior commissure in the opossum: midline extracellular space and glia coincide with early axon decussation. J Neurobiol. 1997; 32:403–414. [PubMed: 9087892]
2. Silver J, Edwards MA, Levitt P. Immunocytochemical demonstration of early appearing astroglial structures that form boundaries and pathways along axon tracts in the fetal brain. J Comp Neurol. 1993; 328:415–436. [PubMed: 8440789]
3. Silver J, Lorenz SE, Wahlsten D, Coughlin J. Axonal guidance during development of the great cerebral commissures: descriptive and experimental studies, in vivo, on the role of preformed glial pathways. J Comp Neurol. 1982; 210:10–29. [PubMed: 7130467]
4. Silver J, Rutishauser U. Guidance of optic axons in vivo by a preformed adhesive pathway on neuroepithelial endfeet. Dev Biol. 1984; 106:485–499. [PubMed: 6500184]
5. Sajin B, Steindler DA. Cells on the edge: boundary astrocytes and neurons. Perspect Dev Neurobiol. 1994; 2:275–289. [PubMed: 7850361]
6. Voigt T. Development of glial cells in the cerebral wall of ferrets: direct tracing of their transformation from radial glia into astrocytes. J Comp Neurol. 1989; 289:74–88. [PubMed: 2808761]
7. Brook GA, Plate D, Franzen R, Martin D, Moonen G, Schoenen J, et al. Spontaneous longitudinally orientated axonal regeneration is associated with the schwann cell framework within the lesion site following spinal cord compression injury of the rat. J Neurosci Res. 1998; 53:51–65. [PubMed: 9670992]
8. Davies SJ, Fitch MT, Memberg SP, Hall AK, Raisman G, Silver J. Regeneration of adult axons in white matter tracts of the central nervous system. Nature. 1997; 390:680–683. [PubMed: 9414159]
9. Davies JE, Huang C, Proschel C, Noble M, Mayer-Proschel M, Davies SJ. Astrocytes derived from glial-restricted precursors promote spinal cord repair. J Biol. 2006; 5:7. [PubMed: 16643674]
10. Leavitt BR, Hernit-Grant CS, Macklis JD. Mature astrocytes transform into transitional radial glia within adult mouse neocortex that supports directed migration of transplanted immature neurons. Exp Neurol. 1999; 157:43–57. [PubMed: 10222107]
11. Tom VJ, Doller CM, Malouf AT, Silver J. Astrocyte-associated fibronectin is critical for axonal regeneration in adult white matter. J Neurosci. 2004; 24:9282–9290. [PubMed: 15496664]
12. Costa S, Planchenault T, Charriere-Bertrand C, Mouchel Y, Fages C, Juliano S, et al. Astroglial permissivity for neuritic outgrowth in neuron-astrocyte cocultures depends on regulation of laminin bioavailability. Glia. 2002; 37:105–113. [PubMed: 11754209]

13. Fallon JR. Preferential outgrowth of central nervous system neurites on astrocytes and Schwann cells as compared with nonglial cells in vitro. J Cell Biol. 1985; 100:198–207. [PubMed: 3880751]
14. Neugebauer KM, Tomaselli KJ, Lilien J, Reichardt LF. N-cadherin, NCAM, and integrins promote retinal neurite outgrowth on astrocytes in vitro. J Cell Biol. 1988; 107:1177–1187. [PubMed: 3262111]
15. Smith GM, Rutishauser U, Silver J, Miller RH. Maturation of astrocytes in vitro alters the extent and molecular basis of neurite outgrowth. Dev Biol. 1990; 138:377–390. [PubMed: 2318341]
16. Tomaselli KJ, Neugebauer KM, Bixby JL, Lilien J, Reichardt LF. N-cadherin and integrins: Two receptor systems that mediate neuronal process outgrowth on astrocyte surfaces. Neuron. 1988; 1:33–43. [PubMed: 2856086]
17. Meiners S, Powell EM, Geller HM. A distinct subset of tenascin/CS-6-PG-rich astrocytes restricts neuronal growth in vitro. J Neurosci. 1995; 15:8096–8108. [PubMed: 8613745]
18. Snow DM, Lemmon V, Carrino DA, Caplan AI, Silver J. Sulfated proteoglycans in astroglial barriers inhibit neurite outgrowth in vitro. Exp Neurol. 1990; 109:111–130. [PubMed: 2141574]
19. Snow DM, Watanabe M, Letourneau PC, Silver J. A chondroitin sulfate proteoglycan may influence the direction of retinal ganglion cell outgrowth. Development. 1991; 113:1473–1485. [PubMed: 1811954]
20. Fawcett JW, Asher RA. The glial scar and central nervous system repair. Brain Res Bull. 1999; 49:377–391. [PubMed: 10483914]
21. Rhodes KE, Moon LD, Fawcett JW. Inhibiting cell proliferation during formation of the glial scar: effects on axon regeneration in the CNS. Neuroscience. 2003; 120:41–56. [PubMed: 12849739]
22. Silver J, Miller JH. Regeneration beyond the glial scar. Nat Rev Neurosci. 2004; 5:146–156. [PubMed: 14735117]
23. Teng YD, Lavik EB, Qu X, Park KI, Ourednik J, Zurakowski D, et al. Functional recovery following traumatic spinal cord injury mediated by a unique polymer scaffold seeded with neural stem cells. Proc Natl Acad Sci USA. 2002; 99:3024–3029. [PubMed: 11867737]
24. Alexander K, Fuss B, Colello RJ. Electric field-induced astrocyte alignment directs neurite outgrowth. Neuron Glia Biol. 2006; 2:93–103. [PubMed: 18458757]
25. Biran R, Noble MD, Tresco PA. Directed nerve outgrowth is enhanced by engineered glial substrates. Exp Neurol. 2003; 184:141–152. [PubMed: 14637087]
26. Sørensen A, Alekseeva T, Katechia K, Robertson M, Riehle MO, Barnett SC. Long-term neurite orientation on astrocyte monolayers aligned by microtopography. Biomaterials. 2007; 28:5498–5508. [PubMed: 17905429]
27. Thompson DM, Buettner HM. Neurite outgrowth is directed by Schwann cell alignment in the absence of other guidance cues. Ann Biomed Eng. 2006; 34:161–168. [PubMed: 16453203]
28. Deumens R, Koopmans GC, Den Bakker CG, Maquet V, Blache S, Honig WM, et al. Alignment of glial cells stimulates directional neurite growth of CNS neurons in vitro. Neuroscience. 2004; 125:591–604. [PubMed: 15099673]
29. Recknor JB, Recknor JC, Sakaguchi DS, Mallapragada SK. Oriented astroglial cell growth on micropatterned polystyrene substrates. Biomaterials. 2003; 25:2753–2767. [PubMed: 14962554]
30. Rajnicek A, Britland S, McCaig C. Contact guidance of CNS neurites on grooved quartz: influence of groove dimensions, neuronal age and cell type. J Cell Sci. 1997; 110:2905–2913. [PubMed: 9359873]
31. Smeal RM, Rabbitt R, Biran R, Tresco PA. Substrate curvature influences the direction of nerve outgrowth. Ann Biomed Eng. 2005; 33:376–382. [PubMed: 15868728]
32. McCarthy KD, de Vellis J. Preparation of separate astroglial and oligodendroglial cell cultures from rat cerebral tissue. J Cell Biol. 1980; 85:890–902. [PubMed: 6248568]
33. Müller HW, Junghans U, Kappler J. Astroglial neurotrophic and neurite-promoting factors. Pharmacol Ther. 1995; 65:1–18. [PubMed: 7716180]
34. Chen MS, Huber AB, van der Haar ME, Frank M, Schnell L, Spillmann AA, et al. Nogo-A is a myelin-associated neurite outgrowth inhibitor and an antigen for monoclonal antibody IN-1. Nature. 2000; 403:434–439. [PubMed: 10667796]

35. Fibrin MT. Myelin-associated inhibitors of axonal regeneration in the adult mammalian CNS. Nat Rev Neurosci. 2003; 4:703–713. [PubMed: 12951563]
36. Jones LL, Sajed D, Tuszynski MH. Axonal regeneration through regions of chondroitin sulfate proteoglycan deposition after spinal cord injury: a balance of permissiveness and inhibition. J Neurosci. 2003; 23:9276–9288. [PubMed: 14561854]
37. McKeon RJ, Jurynec MJ, Buck CR. The chondroitin sulfate proteoglycans neurocan and phosphacan are expressed by reactive astrocytes in the chronic CNS glial scar. J Neurosci. 1999; 19:10778–10788. [PubMed: 10594061]
38. Spencer T, Domeniconi M, Cao Z, Filbin MT. New roles for old proteins in adult CNS axonal regeneration. Curr Opin Neurobiol. 2003; 13:133–139. [PubMed: 12593992]
39. Okada S, Nakamura M, Katoh H, Miyao T, Shimazaki T, Ishii K, et al. Conditional ablation of Stat3 or Socs3 discloses a dual role for reactive astrocytes after spinal cord injury. Nat Med. 2006; 12:829–834. [PubMed: 16783372]
40. Chen CS, Mrksich M, Huang S, Whitesides GM, Inber DE. Geometric control of cell life and death. Science. 1997; 276:1425–1428. [PubMed: 9162012]
41. Clark P, Britland S, Connolly P. Growth cone guidance and neuron morphology on micropatterned laminin surfaces. J Cell Sci. 1993; 105:203–212. [PubMed: 8360274]
42. Théry M, Racine V, Pépin A, Piel M, Chen Y, Sibarita JB, et al. The extracellular matrix guides the orientation of the cell division axis. Nat Cell Biol. 2005; 10:947–953.
43. Théry M, Racine V, Piel M, Pépin A, Dimitrov A, Chen Y, et al. Anisotropy of cell adhesive microenvironment governs cell internal organization and orientation of polarity. Proc Natl Acad Sci USA. 2006; 103:19771–19776. [PubMed: 17179050]
44. Ervasti JM, Campbell KP. A role for the dystrophin-glycoprotein complex as a transmembrane linker between laminin and actin. J Cell Biol. 1993; 122:809–823. [PubMed: 8349731]
45. Hall DE, Reichardt LF, Crowley E, Holley B, Moezzi H, Sonnenberg A, et al. The alpha 1/beta 1 and alpha 6/beta 1 integrin heterodimers mediate cell attachment to distinct sites on laminin. J Cell Biol. 1990; 110:2175–2184. [PubMed: 2351695]
46. Shearer MC, Fawcett JW. The astrocyte/meningeal cell interface--a barrier to successful nerve regeneration? Cell Tissue Res. 2001; 305:267–273. [PubMed: 11545264]
47. Walsh JF, Manwaring ME, Tresco PA. Directional neurite outgrowth is enhanced by engineered meningeal cell-coated substrates. Tissue Eng. 2005; 11:1085–1094. [PubMed: 16144444]
48. Tessier-Lavigne M, Goodman CS. The molecular biology of axon guidance. Science. 1996; 274:1123–1133. [PubMed: 8895455]
49. Ard MD, Bunge RP. Heparan sulfate proteoglycan and laminin immunoreactivity on cultured astrocytes: relationship to differentiation and neurite growth. J Neurosci. 1988; 8:2844–2858. [PubMed: 2970531]
50. Biran R, Webb K, Noble MD, Tresco PA. Surfactant-immobilized fibronectin enhances bioactivity and regulates sensory neurite outgrowth. J Biomed Mater Res. 2001; 55:1–12. [PubMed: 11426386]
51. Zacharias U, Rauch U. Competition and cooperation between tenascin-R, lecticans and contactin 1 regulate neurite growth and morphology. J Cell Sci. 2006; 119:3456–3466. [PubMed: 16899820]
52. Hodgkinson GN, Tresco PA, Hlady V. The differential influence of colocalized and segregated dual protein signals on neurite outgrowth on surfaces. Biomaterials. 2007; 28:2590–2602. [PubMed: 17316787]
53. Kam L, Shain W, Turner JN, Bizios R. Axonal outgrowth of hippocampal neurons on micro-scale networks of polylysine-conjugated laminin. Biomaterials. 2001; 22:1049–1054. [PubMed: 11352086]
54. Yeung CK, Lauer L, Offenhäusser A, Knoll W. Modulation of the growth and guidance of rat brain stem neurons using patterned extracellular matrix proteins. Neurosci Lett. 2001; 301:147–150. [PubMed: 11248444]
55. Gama CI, Tully SE, Sotogaku N, Clark PM, Rawat M, Vaidehi N, et al. Sulfation patterns of glycosaminoglycans encode molecular recognition and activity. Nat Chem Biol. 2006; 2:467–473. [PubMed: 16878128]

56. Tully SE, Mabon R, Gama CI, Tsai SM, Liu X, Hsieh-Wilson LC. A chondroitin sulfate small molecule that stimulates neuronal growth. J Am Chem Soc. 2004; 126:7736–7737. [PubMed: 15212495]

57. Pietak A, McGregor A, Gauthier S, Oleschuk R, Waldman SD. Are micropatterned substrates for directed cell organization an effective method to create ordered 3D tissue constructs? J Tissue Eng Regen Med. 2008; 2:450–453. [PubMed: 18727136]

58. Schnell L, Schwab ME. Axonal regeneration in the rat spinal cord produced by an antibody against myelin-associated neurite growth inhibitors. Nature. 1990; 343:269–272. [PubMed: 2300171]

59. Bradbury EJ, Moon LD, Popat RJ, King VR, Bennett GS, Patel PN, et al. Chondroitinase ABC promotes functional recovery after spinal cord injury. Nature. 2002; 416:636–640. [PubMed: 11948352]

60. Chen MS, Huber AB, van der Haar ME, Frank M, Schnell L, Spillmann AA, et al. Nogo-A is a myelin-associated neurite outgrowth inhibitor and an antigen for monoclonal antibody IN-1. Nature. 2000; 403:434–439. [PubMed: 10667796]

61. McKerracher L, David S, Jackson DL, Kottis V, Dunn RJ, Braun PE. Identification of myelin-associated glycoprotein as a major myelin-derived inhibitor of neurite growth. Neuron. 1994; 13:805–811. [PubMed: 7524558]

62. Williams C, Xie AW, Yamato M, Okano T, Wong JY. Stacking of aligned cell sheets for layer-by-layer control of complex tissue structure. Biomaterials. 2011; 32:5625–5632. [PubMed: 21601276]

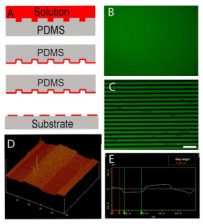

Fig. 1.

Microcontact printing. (A) Casting method for generating patterns of extracellular matrix ligand (red) onto the surface of glass coverslips. (B) Representative fluorescent image of stamped homogeneous laminin (LN) field (green). (C) Representative fluorescent image of micropatterned LN lane pattern consisting of alternating 15 μm wide LN lanes (green) and 15 μm wide lanes of the unpatterned glass coverslip surface (black). (D and E) Representative atomic force microscopy (AFM) image of the topography of a printed LN lane pattern on the glass coverslip. The light color plateaus represent the printed LN lanes and the darker color represents the bare glass coverslip surface. The step height between the printed LN lanes and bare coverslip surface is approximately 5nm as determined by AFM. Scale bar=100 μm.

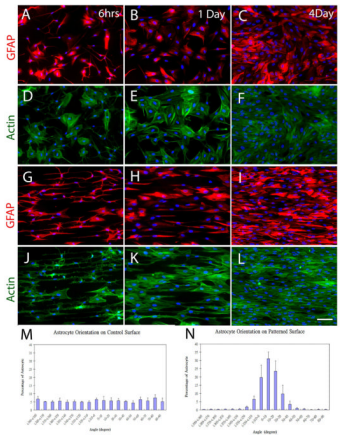

Fig. 2.

Representative astrocyte orientation behavior on homogeneous and patterned LN surfaces stamped on glass coverslips. On homogenous LN fields, astrocytes showed no preferred orientation at 6 hr (A), 1 day (B) and 4 days (C) as visualized with the indirect immunofluorescent histochemistry (IHC) against the intermediate filament Glial Fibrillary Acidic Protein (GFAP) (red), or using fluorescently labeled phalloidin to visualize actin microfilament orientation (D–F). In sharp contrast, the orientation of GFAP (G–I) and fluorescently labeled actin (J–L) on stamped LN lane patterned surfaces revealed considerable anisotropy. A quantitative analysis of astrocyte alignment on homogeneous stamped LN surfaces (M) showed no preferred directionality, whereas a strong bias in the direction of astrocyte alignment on the stamped LN lane patterns (N) was evident. The two groups were significantly different as determined with the Chi Square Test for Independence at a $p < 0.05$. Scale bar= 100 μm.

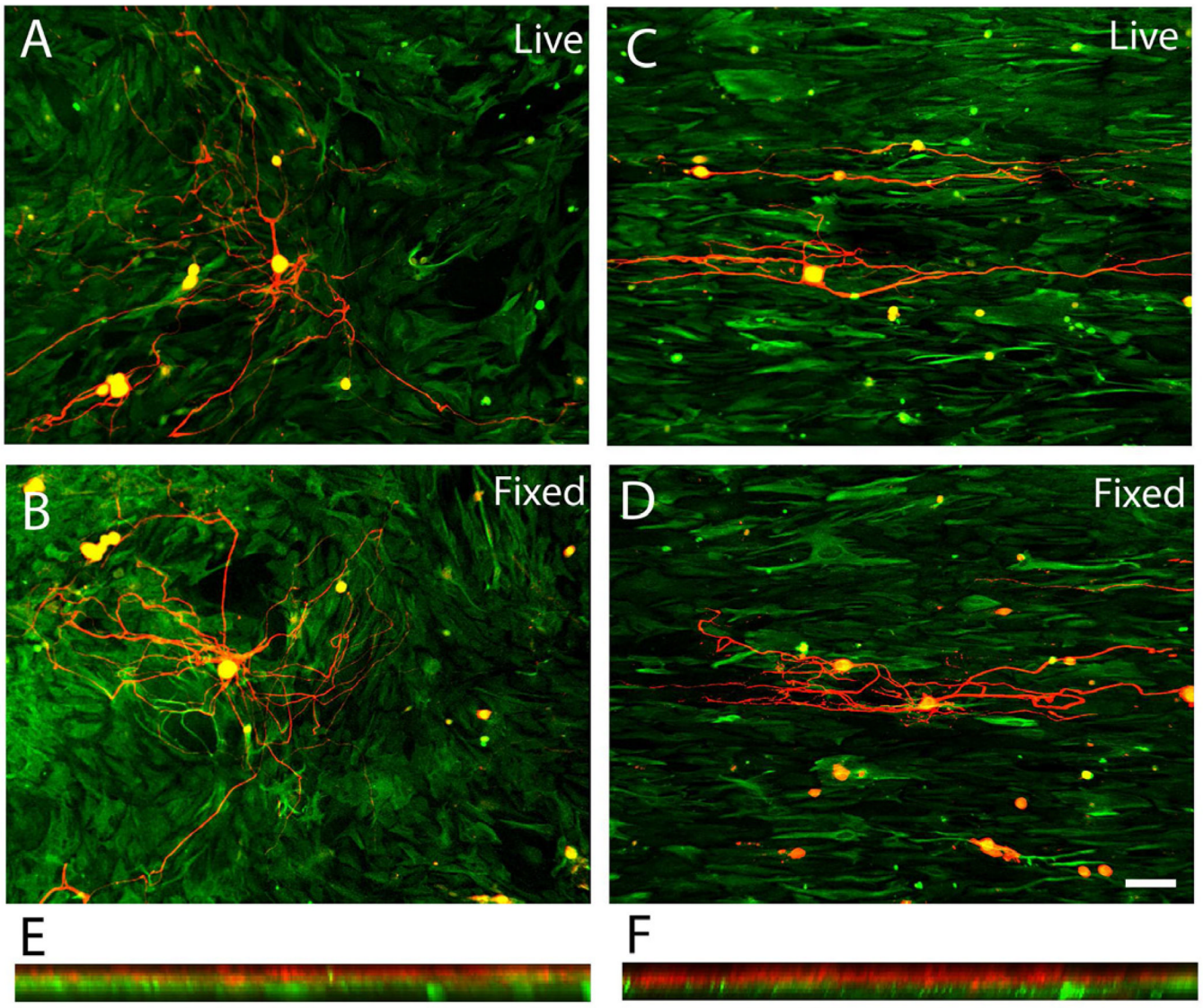

Fig. 3.

Representative confocal images of DRG outgrowth on astrocyte monolayers grown on stamped homogeneous LN fields (left panels) or patterned LN lanes (right panels). (A) Representative DRG outgrowth (red) on live astrocyte monolayers grown on homogeneous LN substrates (GFAP-green) showed no overall preferred directional outgrowth. (B) Similarly, no directionally biased DRG outgrowth was observed on fixed astrocytes cultures grown on homogeneous LN substrates. (C) In sharp contrast, DRG outgrowth on aligned astrocytes monolayers grown on patterned LN substrates extended in the direction of the underlying astrocytes whether alive (C) or fixed (D). Representative, 3D reconstructed confocal images of DRG outgrowth on unaligned astrocytes (E, grown on homogeneous stamped LN) or on aligned astrocyte monolayers (F) demonstrated that DRG outgrowth rarely penetrated into underlying astrocytes and did not reach the surfaces of the stamped coverslips showing that all DRG outgrowth was determined by the interaction with the astrocytes cell layers. Scale bar= 100 μm. Astrocytes were visualized with IHC against GFAP (green) while DRG outgrowth was visualized with antisera directed against neurofilament (red).

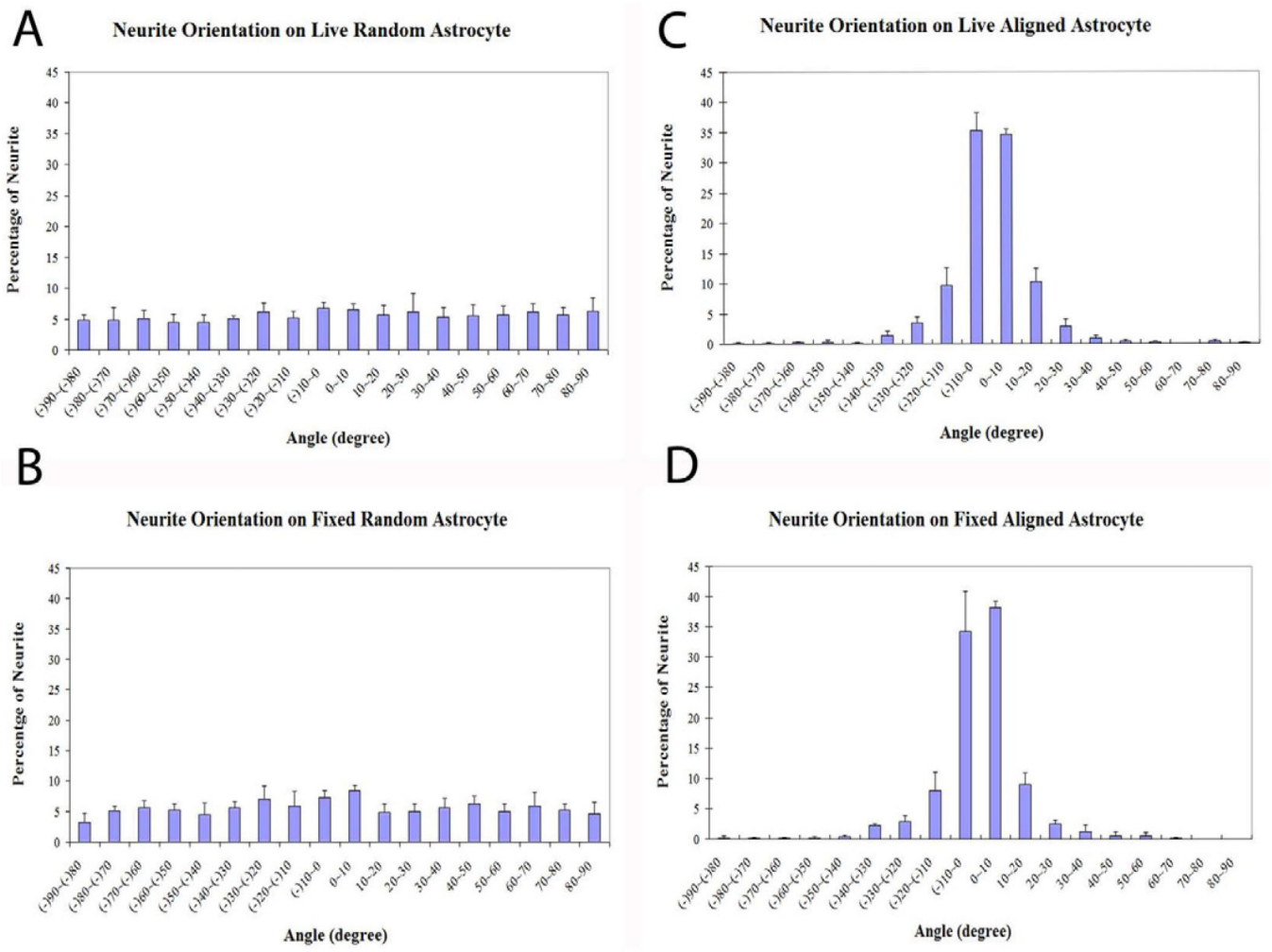

Fig. 4.

Quantitative analysis of DRG outgrowth direction on astrocyte monolayers grown on stamped homogeneous (left panels) or patterned LN surfaces (right panels). The distribution of DRG outgrowth orientation on live (A) and on fixed astrocytes monolayers (B) cultured on homogeneous LN substrates showed no preferred directional outgrowth. In sharp contrast, DRG outgrowth on live (C) or fixed (D) astrocytes grown on patterned LN surfaces showed a strong bias in the direction of the orientation of the underlying astrocytes with a high proportion of neurites growing within 20 degrees parallel to the direction of the orientation of the underlying astrocyte monolayer. The DRG outgrowth direction distribution on astrocyte monolayers grown on patterned surfaces (both live and fixed) was significantly different from those grown on astrocyte monolayers cultured on stamped homogeneous LN fields (both live and fixed) (Chi Square Test for Independence, $p < 0.05$).

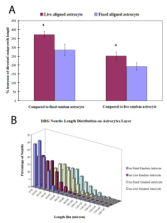

Fig. 5.

Directed neurite outgrowth and directed outgrowth length distributions. (A) DRG outgrowth on oriented astrocytes resulted in greater length in a particular direction (directed outgrowth) where we observed a 370% and 280% increase of the directed length on live and fixed oriented astrocytes monolayers, respectively, compared to that observed on fixed random astrocytes, respectively. When compared to outgrowth on live random astrocytes, the increase of directed outgrowth dropped to 250% and 190%, respectively (ANOVA, $p<0.05$). (B) A comparison of the distribution of directed DRG outgrowth lengths under the four conditions showed that the DRG outgrowth was consistently longer in a larger proportion of the population when the astrocytes monolayers were oriented.

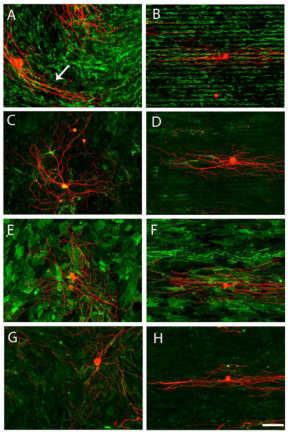

Fig. 6.

Spatial distribution of extracellular matrix molecules expressed by astrocytes and their association with DRG outgrowth on homogeneous LN substrates (left panels) and (patterned LN substrates (right panels). Astrocyte derived FN had a fibrillar structure when grown on homogeneous LN substrates (A) and patterned LN lanes (B). Neurite outgrowth was found to be closely associated with astrocytes derived FN. Although the overall pattern of FN expressed by astrocytes grown on homogeneous LN substrates was not organized, neurite outgrowth tended to follow locally oriented FN fibers (see arrow in panel A). CSPG expression appeared as punctuate expression pattern that was unorganized on the homogeneous LN substrates astrocytes (C) and on aligned astrocytes, as seen with FN (B), appeared to co-align with the underlying pattern of the stamped LN lanes (D). Neurites were found to extend through areas with both high and low expression of CSPG in both culture conditions. The expression of NCAM by both random (E) and aligned astrocyte (F) seemed to delineate astrocyte membranes and act as permissive substrates for neurite to grow. Astrocyte derived LN had similar punctate expression pattern as CSPG on both random (G) and aligned (H) culture and acted as supportive substrates for neurite outgrowth. FN was in green in (A, B); CSPG was in green in (C, D); NCAM was in green in (E, F) and LN was in green in (G, H). Neurites were in red in (A–H). Scale bar=100 μm.

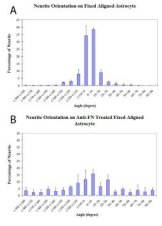

Fig. 7.

Antibodies to astrocyte derived FN attenuated the directed outgrowth of DRGs on aligned astrocytes monolayers. (A) More than 80% of DRG neurite outgrowth on untreated, fixed oriented astrocyte monolayers was observed growing within 20 degrees of the long axis of the orientation of the underlying stamped LN lanes. (B) Following anti-FN antisera treatment, the percentage of neurites within 20 degrees dropped to 46% that was significantly different using the Chi Square Test for Independence at $p<0.05$.

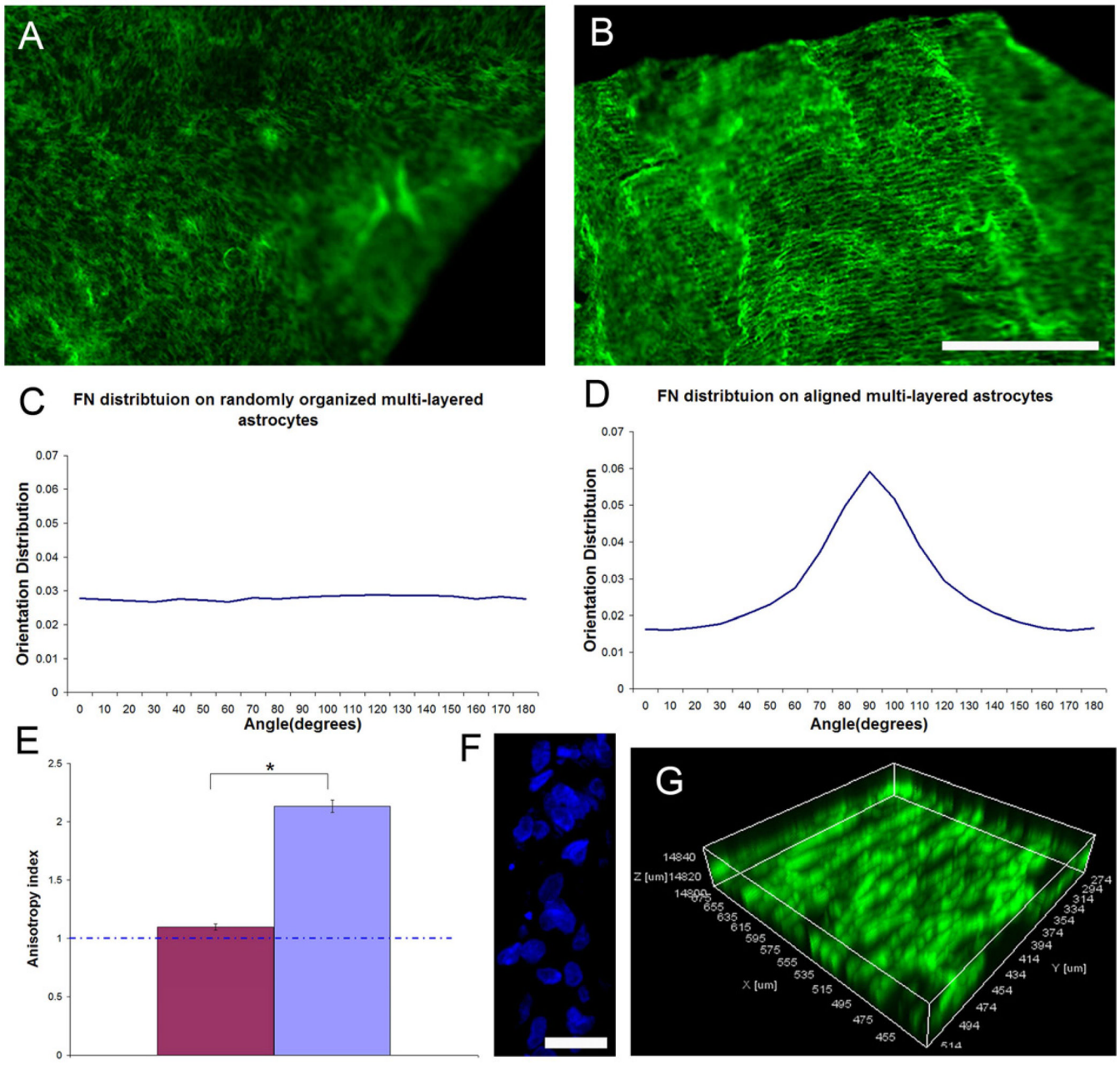

Fig. 8.

The orientation of stamped LN is transferred through multiple cell layers to determine the overall organization of a multilayered astrocyte cell construct. Representative low magnification confocal stacked fluorescent images showing the spatial distribution of FN expressed within a multilayered astrocyte construct gown on a homogeneously stamped LN substrate (A) and on a patterned LN substrate (B) that was mechanically harvested. A 2D FFT analysis on both z-stack confocal images showed that FN orientation distribution on the randomly organized, multilayered astrocyte cultures remained unbiased (C) whereas FN distribution on the aligned, multilayered astrocyte cell constructs peaked around 90 degrees, parallel to the long axis of stamped LN lane pattern (D). (E) An anisotropy index showed that cellular alignment was maintained within the aligned multilayered, astrocyte cell construct (Two-Tailed Student t-Test $p<0.05$). (F) Representative cross-sectional view of the

DAPI stained astrocyte nuclei showing the thickness of the cell construct. (G) Representative 3D reconstructed confocal image showing that the spatial distribution of FN remained aligned throughout the thickness of the astrocyte cell construct grown on a stamped LN substrate. FN was visualized with IHC and is depicted in green in (A, B, G). Scale bar=500 μm in (A, B); =20 μm in (F).